Steric effect on solvation and complexation of metal ions in solution

Shin-ichi Ishiguro

Department of Electronic Chemistry, Tokyo Institute of Technology at Nagatsuta, 4259, Nagatsuta-cho, Midori-ku, Yokohama 227, Japan

<u>Abstract</u> - *N,N*-dimethylformamide (DMF), *N,N*-dimethylacetamide (DMA) and hexamethylphosphoric triamide (HMPA) are all oxygen-donor solvents, and their electron-pair donating property increases in the order DMF ≈< DMA < HMPA. The complexation is thus expected to be generally weakened in the same order of solvents. However, the halogeno complexation of metal ions in DMA and HMPA is significantly enhanced over DMF. Such an unusual complexation cannot be explained in terms of the difference in the strength of metal-solvent bonds, as well as the difference in the strength of ligand-solvent interaction, solvent-solvent interaction in the bulk or nonspecific ion-solvent interaction. Although transition metal(II) ions are six-coordinated in DMA, like DMF, the metal-solvent interaction may be weakened due to an acethyl methyl group next to the coordinating carbonyl oxygen atom. On the other hand, as HMPA is a very bulky molecule, the metal ions can not accommodate six solvent molecules but only four in HMPA. Thus, steric interaction between coordinating solvent molecules plays a key role in the thermodynamic anomaly. Here, thermodynamic and structural aspects of solvation steric effects will be described.

COMPLEXATION OF METAL IONS AND SOLVENT PROPERTIES

The complexation of metal ions in solution depends strongly on the solvent. In general, solvent dielectric constants cannot explain solvent effects on the complexation of metal ions. Especially in coordinating solvents, the strength of metal-solvent bond plays an important role in the solvent effect, as metal-solvent bonds are ruptured upon complexation. Thus, a solvent parameter relating to the strength of an electron-pair donating ability, such as the Gutmann's donor number (ref. 1), may be used to estimate the magnitude of solvent effects on the complexation of relatively hard metal ions. For soft metal ions, a different solvent scale has been proposed by Persson (ref.2).

However, factors other than the strength of direct metal-solvent bonds also play a significant role. Anions tend to form hydrogen bonds, and thus the complexation of anionic ligands is especially weakened in protic or hydrogen-bonding solvents. The complexation is suppressed also in a solvent with a strong solvent-solvent interaction in the bulk (ref. 3). Indeed, the halogeno complexation of metal ions is very weak in water, because the halide ions form hydrogen bonds with water molecules, and besides water molecules in the bulk are strongly interacted with each other to form three dimensional hydrogen-bonded structure. Similarly, the halogeno complexation of metal ions in dimethyl sulfoxide (DMSO) is appreciably weaker than that in DMF, which is mainly due to relatively strong solvent-solvent dipole interaction between DMSO molecules in the bulk (ref. 4-6).

Table 1 shows some physicochemical properties of *N,N*-dimethylformamide (DMF), *N,N*-dimthylacetamide (DMA) and hexamethylphosphoric triamide (HMPA) (ref. 7). They are classified as typical oxygen donor solvents, and their ion-solvent interaction is strong with metal ions but weak with anions. With regard to DMF and DMA, the Gutmann's donor and acceptor

Table 1. Some physicochemical properties of solvents[a]
$$[DMF: HCON(CH_3)_2], \quad [DMA: CH_3CON(CH_3)_2], \quad [HMPA: [(CH_3)_2N]_3PO]$$
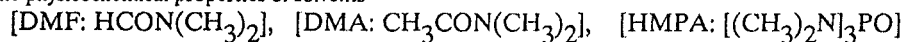
	DMF	DMA	HMPA		DMF	DMA	HMPA
Molecular Weight	73.094	87.121	179.201	Boiling point/°C	153.0	166.1	233
Density/g cm^{-3}	0.944	0.936	1.020	Freezing point/°C	-60.43	-20	7.20
Viscosity/10^{-4} Pa s	8.02	9.27	31.0	Heat of vaporization/J mol^{-1}	47.514	49.15	61.1
Heat capacity/J K^{-1} g^{-1}	148.36	151.4	321.3	Dipole moment/10^{-30} C m	10.80[b]	14.23[c]	18.47[b]
Donor number (DN)	26.6	27.8	38.8	Dielectric constant	36.71	37.78	29.30[d]
Acceptor number (AN)	16.0	13.6	10.6				

[a]Values refer to 25 °C and 1.0132×10^{-5} Pa. [b]in benzene. [c]in 1,4-dioxane. [d]20 °C.

numbers are not significantly different, as well as other solvent properties such as density, viscosity and dielectric constant. With HMPA, viscosity is higher and dielectric constant is slightly smaller than that of DMF. The donor and acceptor numbers suggest that HMPA acts as a stronger donor but weaker acceptor compared to DMF.

Unlike water, aprotic solvents DMF and DMA have no ability to form hydrogen bonds, and besides their solvent-solvent interaction in the bulk is weak. This leads to a significantly enhanced halogeno complexation of metal ions in these aprotic solvents over water. However, despite the similar electron-pair donating and accepting properties of DMF and DMA, thermodynamics of metal complexation in these solvents is quite different. The complexation in HMPA is also unusual. Evidently, the steric interaction between coordinating solvent molecules to a metal ion play a key role in the anomaly. Here, we compare thermodynamics and structure of metal complexes in DMF, DMA and HMPA with a special attention to the steric interaction on solvation and complexation in DMA and HMPA.

Table 2. Thermodynamic parameters of the stepwise chloro complexation in dimethylformamide and dimethylacetamide containing 0.4 mol dm^{-3} Et$_4$NClO$_4$ and 0.1 mol dm^{-3} Et$_4$NBF$_4$, respectively, at 25 °C.

	Dimethylformamide				Dimethylacetamide			
	Mn[a]	Co[a]	Ni[b]	Zn[b]	Mn[c]	Co[c]	Ni[d]	Zn[c]
$\log K_1$	3.69	3.43	2.85	4.81	4.1	5.42	4.31	8.6
$\log K_2$	2.40	3.42	0.91	6.99	3.9	6.42	4.22	7.8
$\log K_3$	3.93	4.99	1.77	5.26	4.3	4.45	4.51	5.0
$\log K_4$	2.61	2.29	1.87	2.22	2.12	1.97	1.73	1.94
ΔH_1°	1.1	6.3	8.6	14.7	18.6	26	28.4	-1.7
ΔH_2°	25.6	52.2	19.1	1.4	16	-4	22	-20.6
ΔH_3°	5.1	-24.8	62.9	-17.6	-13	-13.6	-3.3	-16.9
ΔH_4°	-10.5	-6.1	-13.4	-7.9	-12.3	-7.5	-6.4	-10.4
ΔS_1°	74	87	84	142	141	190	178	159
ΔS_2°	132	241	82	139	126	111	154	80
ΔS_3°	92	12	245	42	38	40	75	39
ΔS_4°	15	23	-9	16	-1	12	12	2
$\Delta G_{\beta 4}^\circ$	-72.1	-80.6	-42.2	-110.0	-82	-104.2	-84.3	-133
$\Delta H_{\beta 4}^\circ$	21.3	27.6	77.2	-9.4	8.5	1.2	40.7	-49.6
$\Delta S_{\beta 4}^\circ$	313	363	401	338	305	354	419	281

[a]ref. 8, [b]ref. 9, [c]ref. 10, [d]ref. 11. $\log(K/\text{mol}^{-1}\ \text{dm}^3)$, $\Delta H^\circ/\text{kJ mol}^{-1}$ and $\Delta S^\circ/\text{J K}^{-1}\ \text{mol}^{-1}$.
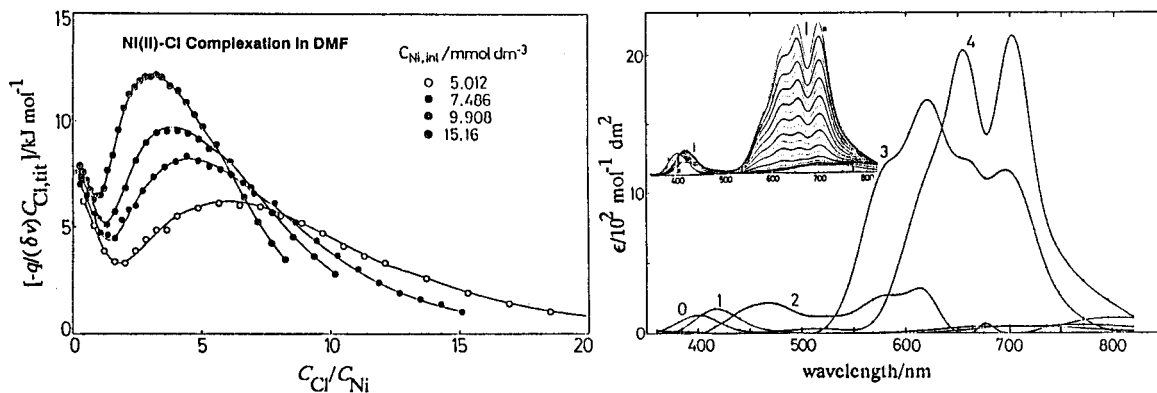

Fig. 1. (a) Calorimetric titration curves for the nickel(II)-chloride system in DMF containing 0.4 mol dm^{-3} Et$_4$NClO$_4$ at 25 °C, (b) Electronic spectra of individual [NiCl$_n$]$^{(2-n)+}$ (n = 1-4) complexes.

THERMODYNAMICS OF COMPLEXATION IN DMF AND DMA

The chloro complexation of transition metal(II) ions and some lanthanide(III) ions have been studied in DMF and DMA by a precise titration calorimetry system developed in our laboratory. Fig. 1(a) shows typical calorimetric titration curves obtained for the nickel(II)-chloride system in DMF. The heat of reaction q measured is normalized as $[-q/(\delta v)C_{Cl,tit}]$, where δv and $C_{Cl,tit}$ stand for the volume of the added titrant and the concentration of the chloride ion in the titrant, respectively, and is plotted against C_{Cl}/C_{Ni} in solution. The calorimetric data were analyzed by a nonlinear least-squares program, and the titration curves were well explained in terms of the formation of $[NiCl_n]^{(2-n)+}$ ($n = 1$-4) complexes (ref.9). In fact, the solid lines, calculated by using the formation constants, reaction enthalpies and entropies thus obtained, reproduce well all the experimental points. The formation constants of the complexes were also obtained by spectrophotometric titration and electronic spectra of individual complexes were extracted as shown in Fig. 1(b). Thermodynamic parameters for the chloro complexation of manganese(II), cobalt(II), nickel(II) and zinc(II) ions are listed in Table 2. The species distribution is shown in Fig. 2. It clearly demonstrates that, in all the metal systems examined, the complexation is significantly favorable in DMA compared to DMF. The variation of stepwise enthalpy and entropy values depends strongly on the metal ion. The $\Delta S^\circ_{\beta 4}$ values for the overall formation of $[MCl_4]^{2-}$ are all large and positive, which is typical in strong donor solvents.
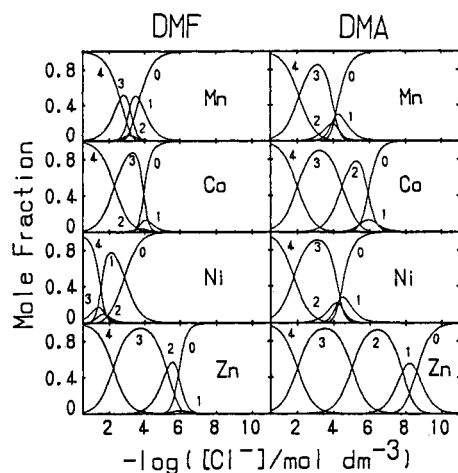

Fig.2. Species distribution of chloro complexes of transition metal(II) ions in DMF and DMA at 25° C. The number represents n within $[MCl_n]^{(2-n)+}$.
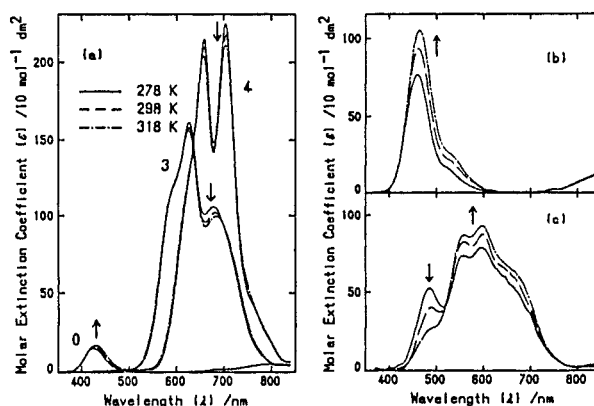
Fig.3. Extracted electronic spectra of $[NiCl_n]^{(2-n)+}$ ($n = 1$-4) in DMA. (a) The number represents n within $[NiCl_n]^{(2-n)+}$ ($n = 0, 3$ and 4), (b) $[NiCl]^+$, and (c) $[NiCl_2]^0$.

A significant difference was also found for the halogeno complexation of lanthanide(III) ions in DMF (ref.12) and DMA. The monochloro and monobromo complexes are appreciably formed and their formation constants, enthalpies and entropies were obtained calorimetrically in both the solvents, although the measurements in DMA are still going on. For instance, in DMF the ΔH°_1 value for $[LaCl]^{2+}$ is 21.2 kJ mol^{-1}, which is significantly more positive than the value of 5 kJ mol^{-1} for $[LaBr]^{2+}$. This is unexpected considering that the lanthanide(III) ions are classified as hard metal ions. Interestingly, such an unusual complexation behavior cannot be observed in DMA, i.e., the ΔH°_1 values are 19.1 and 25 kJ mol^{-1} for chloride and bromide, respectively. Note that the corresponding entropy values are large and positive except for the complexation of $[LaBr]^{2+}$ in DMF, suggesting that chloride ions form inner-sphere complexes in both the solvents, while bromide ions form inner complexes in DMA but outer complexes in DMF. The yttrium(III) ion behaves as lanthanide(III) ions, and the ^{89}Y NMR of bromide solutions shows no chemical shift relative to that of a perchlorate solution of DMF, while the corresponding NMR shows a significant shift in DMA, providing evidence of the outer- and inner-sphere bromo complexation in DMF and DMA, respectively (ref.13).

COORDINATION GEOMETRY CHANGE UPON COMPLEXATION

In DMF, green color of a nickel(II) perchlorate solution changes to deep blue upon addition of a tetraethylammonium chloride solution. This implies that an octahedral six-coordinate geometry around nickel(II) ion changes to a tetrahedral four-coordination upon complexation. The electronic spectra clearly demonstrate that the mono- and dichloro complexes are six-coordinated, but the tri- and tetrachloro complexes are four-coordinated. We can thus conclude that the coordination geometry changes at the third step of complexation (Scheme 1). The coordination geometry change is accompanied by extensive liberation
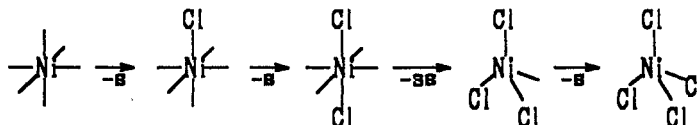

Scheme 1 (S = DMF)

of bound solvent molecules. In fact, in Table 2, the ΔH°_3 and ΔS°_3 values for the Ni(II)-Cl system in DMF are particularly large and positive, suggesting that solvent molecules bound to metal ions are liberated extensively upon the formation of $[NiCl_3]^-$. Similarly, for the Co(II)-Cl system in DMF, both thermodynamic parameters and electronic spectra show that an O_h-T_d geometry change occurs at the second step. With manganese(II) in DMF, large and positive enthalpy and entropy values appear at the second step like cobalt(II). With zinc(II), the formation of $[ZnCl]^+$ is strongly suppressed, and the geometry change thus occurs upon the formation of $[ZnCl_2]^0$.

In DMA, on the other hand, the ΔH°_1 and ΔS°_1 values are large and positive in all the metal systems examined, suggesting that extensive liberation of bound solvent molecules occurs at the first step of complexation. According to the extracted electronic spectra (Fig.3), the free nickel(II) ion is evidently six-coordinated, while the tri- and tetrachloro complexes are four-coordinated (ref.13). With respect to the mono- and dichloro complexes, electronic spectra show thermochromism, suggesting that solvation equilibria between five- and six-coordination for $[NiCl]^+$ and between four- and five-coordination for $[NiCl_2]^0$ are established (scheme 2).

In general, the coordination geometry change upon complexation occurs at an earlier step in DMA than in DMF. This applies also for the isothiocyanato complexes of nickel(II). In both DMF and DMA, a series of mono-, di-, tri- and tetraisothiocyanato complexes are formed. Interestingly, no coordination geometry change occurs upon complexation in DMF (ref.14), while it does upon the formation of the tetraisothiocyanato complex in DMA.
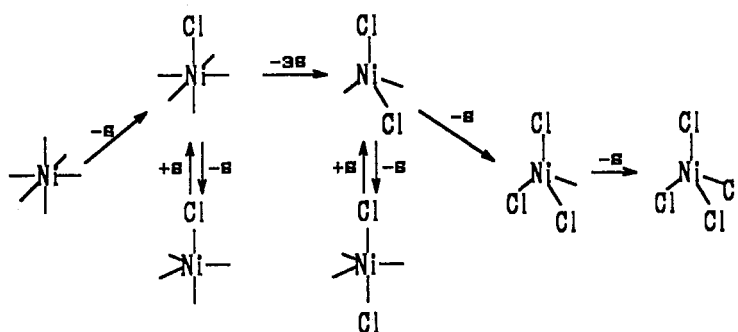
Scheme 2 (S = DMA)

STRUCTURAL PARAMETERS IN SOLUTION

EXAFS measurements provide information on the coordination structure around metal ions in solution. The structural parameters of metal solvates in DMF and DMA are listed in Table 3, along with those in HMPA. For Mn(II), Co(II), Ni(II) and Zn(II) in DMF (ref. 15,16), all n values are close to 6, and the r values are practically the same as those of the corresponding hydrates, indicating that these metal ions are octahedrally six-coordinated as in water (ref. 17). This applies also for Mn(II), Co(II) and Ni(II) in DMA (ref. 16). In Table 2, with Mn(II), Co(II) and Ni(II), the $\Delta S^\circ_{\beta_4}$ value in DMA is similar to that in DMF, while the $\Delta H^\circ_{\beta_4}$ value in DMA is appreciably smaller than that in DMF. As the solvation of the anionic $[MCl_4]^{2-}$ complex may be weak and to a similar extent in both DMF and DMA, the smaller $\Delta H^\circ_{\beta_4}$ value might reflect weaker solvation of metal ions within $[M(DMA)_6]^{2+}$. We thus imagine that the M-O(DMA) bonds are deformed due to steric hindrance of the acethyl methyl groups between the octahedrally coordinated DMA molecules.

With regard to Zn(II) in DMA, an appreciably small n and r values were observed, indicating that an octahedral geometry is not kept in this system. The M-O(DMA) bond is shortened with reduced solvation number. Consequently, desolvation upon complexation may be less extensive, as indicated by the $\Delta S^\circ_{\beta_4}$ value, which is markedly smaller in DMA than in DMF.

Table 3. The solvation number, n, and M-O(solvent) bond length, r/pm, of metal(II) ions in dimethylformamide, dimethylacetamide and hexamethylphosphoric triamide.

	DMF		DMA		HMPA	
	n	r	n	r	n	r
Mn(II)	5.8	216	5.8	216	4.9	207
Co(II)	5.9	208	5.5	207	3.9	195
Ni(II)	5.9	204	5.9	205	4.2	197
Zn(II)	5.8	208	4.6	199	4.1	193
Cd(II)					4.8	223

Lanthanide(III) ions can accommodate eight or nine solvent molecules. The crystal ionic radii of lanthanide(III) ions decrease monotonically with the atomic number. Our recent EXAFS study (ref.18) revealed that the M-O(DMA) bond length is shorter than the M-O(DMF) one, and the shortening is more pronounced with the atomic number as shown in Fig. 4. This suggests that the steric interaction between coordinated solvent molecules is more pronounced for a metal ion with a smaller ionic radius. As expected, the halogeno complexation of lanthanide(III) ions is considerably enhanced in DMA over DMF.

As described in a previous section, it was suggested that lanthanide(III) ions form outer-sphere complexes with bromide ions in DMF, while inner-sphere complexes in DMA. The direct structural evidence was obtained by EXAFS as shown in Fig. 5, in which the Fourier Transforms $F(r)$ extracted from EXAFS spectra are compared. As the $F(r)$ shows a radial distribution of atoms around the thulium(III) ion, the peak around 200 pm for a $Tm(ClO_4)_3$ DMF or DMA solution is evidently due to the metal-O(solvent) interaction. Practically the same profile of $F(r)$ was obtained for a $TmBr_3$ DMF solution, i.e., no bromide ion coordinates to the metal ion in DMF. In contrast, an additional peak corresponding to the metal-Br interaction was found for a $TmBr_3$ DMA solution, which clearly indicating that bromide ions coordinate to lanthanide(III) ions in DMA.
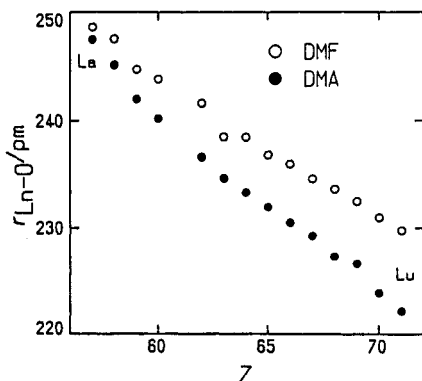

Fig. 4. Variation of the M-O bond length of solvate ions of lanthanide(III) in DMF and DMA solutions.
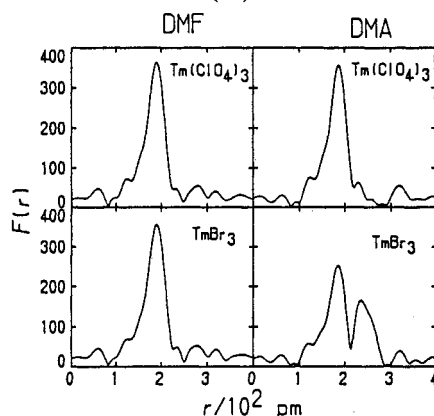
Fig. 5. The Fourier transforms $F(r)$ of the extracted EXAFS curves for Tm(III) in DMF and DMA.

COMPLEXATION AND STRUCTURE IN HMPA

HMPA is an oxygen donor solvent, but the metal(II) perchlorate solvate crystals involve only four HMPA molecules per a metal ion. In fact, the cobalt(II) perchlorate show deep blue color in HMPA and in the solid state, indicating that the metal ion is tetrahedrally four-coordinated. The small solvation number compared to that in other oxygen donor solvents is evidently due to the steric interaction between bulky HMPA molecules.

Thermodynamic parameters for the halogeno complexation of the cobalt(II) ion in HMPA are shown in Table 4, together with those for the zinc(II) and cadmium(II) systems. The species distribution for the cobalt(II) halide systems is shown in Fig. 6 as a typical example. As no geometry change occurs upon complexation in HMPA, four HMPA molecules are stepwise replaced with

Table 4. Thermodynamic parameters of the stepwise halogeno complexation in hexamethylphosphoric triamide containing 0.1 mol dm^{-3} Bu$_4$NClO$_4$ at 25 ° C.

	Cobalt(II)[a]			Zinc(II)[b]			Cadmium(II)[c]	
	Cl	Br	I	Cl	Br	I	Br	I
log K_1	6.7	5.6	2.7	9.5	6.7	4.1	9.3	7.2
log K_2	4.2	3.2	0.9	6.5	3.9	1.54	7.0	5.4
log K_3	2.7	0.8		3.6			4.5	2.26
log K_4	(0.8)			2.3			1.9	
ΔH_1°	-15.2	-2.7	13.0	-20.0	-7.7	7.3	0.6	14.7
ΔH_2°	-12.6	0.3	6.9	-15.2	-3.4	9.8	-5.6	-4.9
ΔH_3°	-12.8	2.1		-11.6			-18.4	-12.2
ΔH_4°	(-8)			-3.4			-5.7	
ΔS_1°	78	97	95	115	101	102	177	189
ΔS_2°	38	62	40	74	63	62	116	86
ΔS_3°	9	22		31			25	10
ΔS_4°	(-10)			32			15	

[a] ref. 19, [b] ref. 20, [c] ref. 21. log(K/mol^{-1} dm^3), ΔH°/kJ mol^{-1} and ΔS°/J K^{-1} mol^{-1}.
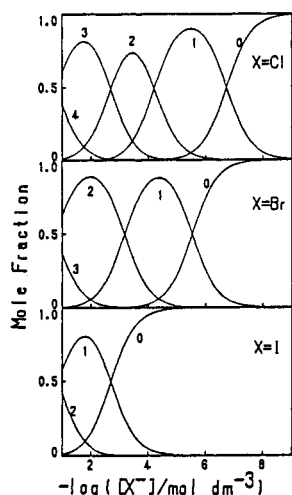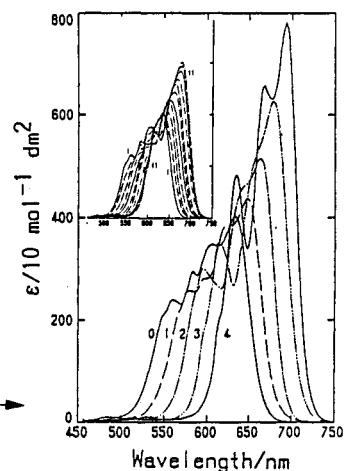
Fig.6. Species distribution of the halogeno complexes of cobalt(II) in HMPA at 25° C.

Fig.7. Electronic spectra of $[CoCl_n]^{(2-n)+}$ complexes in HMPA at 25° C.

chloride ions to form extensively the mono-, di-, tri- and tetrachloro complexes with increasing concentration of the chloride ion in solution. Electronic spectra of individual cobalt(II) chloride complexes are shown in Fig. 7. Unlike DMF and DMA, the stepwise reaction enthalpies are all negative in HMPA.

Thermodynamics of complexation for the zinc(II) system show a similar trend to that for the cobalt(II) systems. Indeed, the ΔH°_1 and ΔH°_2 values for the Zn(II)-Cl, -Br and -I systems are systematically more negative by ca. 5 and 3 kJ mol^{-1} than the corresponding Co(II) systems.

However, a question arises that why are the ΔH°_1 values for [CoCl]$^+$ and [ZnCl]$^+$ negative in HMPA. The result is surprising because the corresponding values in DMF are positive. Note that in both solvent one metal-solvent bond is replaced with one metal-chloride bond, and that the electron-pair donating ability of HMPA is stronger than that of DMF. In Table 3, the M-O(HMPA) bond length is significantly shortened compared to the corresponding M-O(DMF) bond, indicating that the M-O bond is strengthened in HMPA. Although the structural parameters for [CoCl(DMF)$_5$]$^+$ can not be determined due to its suppressed formation in DMF, what applies for water may also apply for DMF. The Co-O and Co-Cl bond lengths within [CoCl(H$_2$O)$_5$]$^+$ are 214 and 235 pm, respectively. The corresponding values within [CoCl(HMPA)$_3$]$^+$ are 195 and 224 pm. Indeed, the Co-Cl bond length in HMPA is shorter than that in water. In addition, the Co-O(H$_2$O) bond within [CoCl(H$_2$O)$_5$]$^+$ is elongated compared to that of [Co(H$_2$O)$_6$]$^{2+}$ (208pm), but the Co-O(HMPA) bond length does not appreciably change upon complexation. Accordingly, both Co-O and Co-Cl bonds are responsible more or less to the thermodynamic anomaly of complexation in HMPA and DMF.

The complexation behavior of the cadmium(II) ion is markedly different from that of the cobalt(II) ion, i.e., $\Delta H^\circ_1 > \Delta H^\circ_2$ for Cd(II) in contrast to $\Delta H^\circ_1 < \Delta H^\circ_2$ for Co(II). Besides, the ΔS°_1 value are considerably larger. This suggests that the relatively large cadmium(II) ion can accommodate more than four HMPA molecules. Indeed, the average coordination number $n = 4.8$ and the r value of 223 pm were obtained in neat HMPA. The n value decreases upon dilution of HMPA with inert nitromethane, and in nitromethane rich solution, the n value is 3.9 with the r value of 217pm, suggesting the presence of a solvation equilibrium between four- and five-coordination in HMPA.

REFERENCES

1. V. Gutmann, "The Donor-Acceptor Approach to Molecular Interactions," Prenum, New York (1978).
2. I. Persson, Pure Appl. Chem., 58, 1153-1161 (1986).
3. S. Ahrland, Pure Appl. Chem., 51, 2019-2039 (1979).
4. H. Suzuki, S. Ishiguro and H. Ohtaki, J. Chem. Soc. Faraday Trans. 1, 85, 2587-2596 (1989).
5. H. Suzuki, S. Ishiguro and H. Ohtaki, J. Chem. Soc. Faraday Trans., 86, 2179-2185 (1990).
6. S. Ishiguro, H. Suzuki, B. G. Jeliazkova and H. Ohtaki, Bull. Chem. Soc. Jpn., 62, 39-44 (1989).
7. J. A. Riddick, W. B. Bunger and T. K. Sakano, "Organic Solvents," John Wiley & Sons, New York (1986)
8. S. Ishiguro, K. Ozutsumi and H. Ohtaki, J. Chem. Soc. Faraday Trans. 1, 84, 2409-2419 (1988).
9. S. Ishiguro, K. Ozutsumi and H. Ohtaki, Bull. Chem. Soc. Jpn., 60, 531-538 (1987).
10. H. Suzuki, M. Koide and S. Ishiguro, To be published.
11. H. Suzuki and S. Ishiguro, Inorg. Chem., 31, 4178-4183 (1992).
12. S. Ishiguro and R. Takahashi, Inorg. Chem., 30, 1854-1858 (1991).
13. R. Takahashi and S. Ishiguro, J. Chem. Soc. Faraday Trans., 87, 3379-3383 (1991).
14. S. Ishiguro and K. Ozutsumi, Inorg. Chem., 29, 1117-1123(1990).
15. K. Ozutsumi, K. Tohji, Y. Udagawa and S. Ishiguro, Bull. Chem. Soc. Jpn., 64, 1528-1532 (1991).
16. K. Ozutsumi, H. Suzuki, M. Koide and S. Ishiguro, J. Phys. Chem., in press.
17. H. Ohtaki, Rev. Inorg. Chem., 4, 103-177 (1982)
18. R. Takahashi, K. Ozutsumi and S. Ishiguro, To be published.
19. Y. Abe, K. Ozutsumi and S. Ishiguro, J. Chem. Soc. Faraday Trans. 1, 85, 3747-3756 (1989).
20. Y. Abe and S. Ishiguro, J. Solution Chem., 20, 793-803 (1991).
21. Y. Abe, R. Takahashi, S. Ishiguro and K. Ozutsumi, J. Chem. Soc. Faraday Trans., 88, 1997-2002 (1992).